Design of a New Haptic Device using a Parallel Mechanism with a Gimbal Mechanism

Sung-Uk Lee*, Hochul Shin** and Seungho Kim***

Nuclear Robotics Lab, Korea Atomic Energy Research Institute, Daejeon, Korea

* (Tel : +82-42-868-8885; E-mail: sulee@kaeri.re.kr)

** (Tel : +82-42-868-8836; E-mail: smarthc@kaeri.re.kr)

***(Tel : +82-42-868-2928; E-mail: robotkim@kaeri.re.kr)

Abstract: This paper proposes a new haptic device using a parallel mechanism with gimbal type actuators. This device has three legs actuated by 2-DOF gimbal mechanisms, which make the device simple and light by fixing all the actuators to the base. Three extra sensors are placed at passive joints to obtain a unique solution of the forward kinematics problem. The proposed haptic device is developed for an operator to use it on a desktop in due consideration of the size of an average Korean. The proposed haptic device has a small workspace for on operator to use it on a desktop and more sensitivity than a serial type haptic device. Therefore, the motors of the proposed haptic device are fixed at the base plate so that the proposed haptic device has a better dynamic bandwidth due to a low moving inertia. With this conceptual design, optimization of the design parameters is carried out. The objective function is defined by the fuzzy minimum of the global design indices, global force/moment isotropy index, global force/moment payload index, and workspace. Each global index is calculated by a SVD (singular value decomposition) of the force and moment parts of the jacobian matrix. Division of the jacobian matrix assures a consistency of the units in the matrix. Due to the nonlinearity of this objective function, Genetic algorithms are adopted for a global optimization.

Keywords: Haptic Device, Parallel Mechanism, Gimbal Mechanism, Optimal Design

1. INTRODUCTION

In doing some tasks remotely, one operator generally has visual and audible information about the working environment. When the teleoperation task requires contact between the end-effector and the environment, this information is not sufficient. For such a task, a force reflecting master may help the operator get some important information about a contact with the environment. A force reflecting bilateral universal master, a simple haptic device, can transmit data from an operator to a slave, a slave to an operator, or in both directions.

Researches about haptic devices began in the 1950s, when a master-slave system was proposed by Goertz [1]. Since then, many haptic devices have been developed. Bergamasco [2] proposed an exoskeleton type master an arm which can display an arm motion within a large workspace. But it was too heavy and a practical realization is difficult. Phantom [3] developed by Massie and Salisbury is a serial type 3DOF haptic device, which is not enough to display the real environment. And serial structures can not display a hard contact feeling.

Comparing a serial mechanism to a parallel one, it has many advantages, in spite of a smaller workspace, more difficulty in solving the forward kinematics. It has a high stiffness and high accuracy because of its closed structure. Using a parallel mechanism in a haptic device has several merits due to the characteristics of the parallel mechanism. Contrary to the serial mechanism, the inertia, which is a major cause for an operator's fatigue, can be mitigated since the actuator can be attached to the base plate in a parallel mechanism. And, a higher stiffness guarantees the mechanical stability of the device, and a high bandwidth.

Haptic devices using a parallel mechanism have been proposed by many researchers. Woo [4] developed kaist master 1 using a fivebar parallel mechanism. It has a compact size, large workspace, high mechanical rigidity, but the actuators are floated. Due to the floating actuators, it has a relatively large inertia. Yoon [5] proposed a mechanism composed of three pantograph mechanisms, which has motors fixed at the base for a better dynamic bandwidth owing to a low moving inertia and it has a wider orientation workspace due to a RRR type spherical joint. New parallel mechanism was proposed by Lee [6], which is light by employing a non-floating actuator and has a relatively large orientation workspace. Haptic devices using a parallel mechanism with a gimbal were developed by Tsumaki [7] and Yi [8]. Tsumaki proposed a modified Delta mechanism with a fivebar gimbal mechanism which is a 3-DOF spatial orientation mechanism. It has a compact size and a large orientation workspace, but the spatial gimbal mechanism has three floating actuators. These make the moving inertia large. Yi developed a 4-legged parallel manipulator which has 4 actuating 2-DOF gimbals fixed at the base.

This paper presents a haptic device using a parallel mechanism with a gimbal structure. Gimbal structure has two rotary actuators mounted on the base. Owing to the 2-DOF gimbal, the moving inertia of this device is reduced drastically. An additional three sensors with six actuator sensors make it possible to establish a simple closed form solution of the forward kinematics. The reference axis of the gimbal mechanism is rotated about the z axis with 45 degrees. Due to this rotation, this device can distribute the end-effector load to each actuator uniformly. This paper consists of an analysis of the kinematics and performance, as well as the optimal design. Analysis section includes an inverse/forward kinematics and screw based Jacobian matrix analysis. In the optimal design section, there are definitions of the performance index, such as the isotropy index and payload index. And a design parameter optimization is performed with a global design index which is defined with a global isotropy index and a global payload index.

2. CONCEPTUAL DESIGN

In designing a new haptic device, the followings are considered.

- 6 dof
- Reachable workspace considering human factor
- Less fatigue during operation
  - Low inertia, light moving part and low friction.

Firstly, a reachable workspace is defined by considering human factor. On the assumption that an operator use a haptic device on a desktop, the reachable workspace is selected as Fig.1, in due consideration of the size of an average Korean.

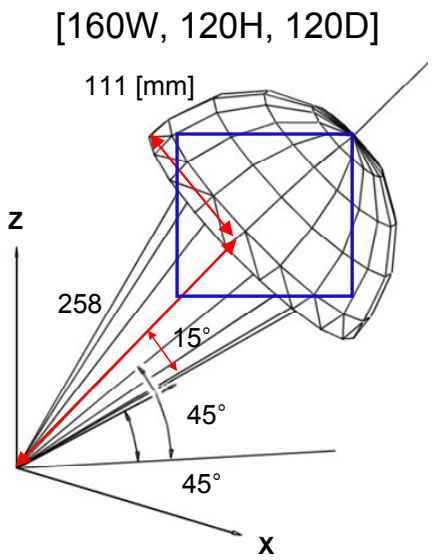

Fig. 1 The reachable workspace dimension

Finally, a parallel mechanism and a gimbal mechanism are considered as the main mechanisms of the proposed haptic device for a lesser fatigue during on operation. A gimbal mechanism makes it possible to fix actuators to the base plate, so that the inertia of the proposed haptic device is low. Because all the actuators are located in the base plate and the 2 dof gimbal mechanism, it makes the moving part of the proposed haptic device light. A parallel mechanism has many advantages in spite of a smaller workspace. It has a high stiffness, high bandwidth and high accuracy. In order that the proposed haptic device has 6 dof, the three 2 dof gimbal mechanism and three legs are used. Fig. 2 shows the conceptual design of the proposed haptic device.

In addition, an additional three angle sensors is used to establish a simple closed form solution of the forward kinematics of the proposed haptic device.

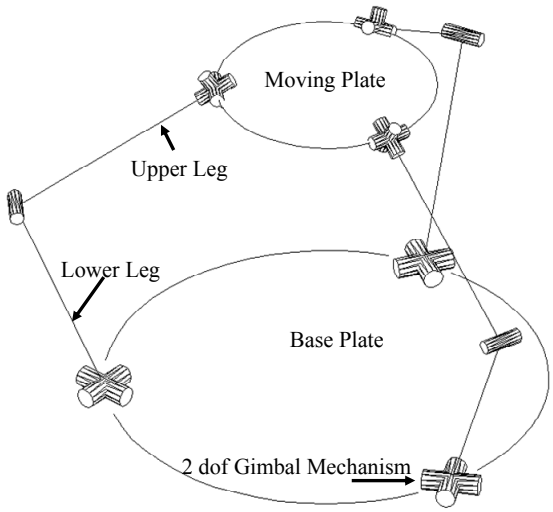

Fig. 2 The conceptual design of the proposed haptic

3. KINEMATICS ANALYSIS

In this section, the kinematics of the proposed haptic device is analyzed to calculate the mechanical parameters.

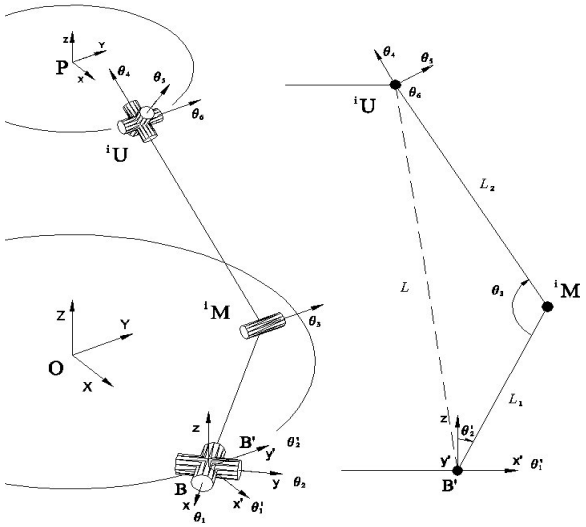

Fig. 3 The definition of the virtual frame

3.1 Forward position analysis

Generally, it is not easy to get a closed form solution for a forward kinematics problem of a parallel mechanism. But this mechanism has 3 redundant sensors at the middle revolute joints. These sensors make it easy to solve the forward kinematics problem. For simplicity, virtual frame B' is aligned to be parallel to base frame O. Each homogeneous transformation matrix is expressed as below.

$$
{}^{\mathrm{O}}_{\mathrm{B}}\mathbf{T} = \begin{bmatrix} \mathrm{c}\left(120\left(i-1\right)\right) & -\mathrm{s}\left(120\left(i-1\right)\right) & 0 & Rb\mathrm{c}\left(120\left(\mathrm{i}\text{-}1\right)\right) \\ \mathrm{s}\left(120\left(\mathrm{i}\text{-}1\right)\right) & \mathrm{c}\left(120\left(\mathrm{i}\text{-}1\right)\right) & 0 & Rb\mathrm{s}\left(120\left(\mathrm{i}\text{-}1\right)\right) \\ 0 & 0 & 1 & 0 \\ 0 & 0 & 0 & 1 \end{bmatrix},
$$

$$
{}^{\mathrm{B}}_{\mathrm{B}'}\mathbf{T} = \begin{bmatrix} \mathrm{c}\left(-45^\circ\right) & -\mathrm{s}\left(-45^\circ\right) & 0 & 0 \\ \mathrm{s}\left(-45^\circ\right) & \mathrm{c}\left(-45^\circ\right) & 0 & 0 \\ 0 & 0 & 1 & 0 \\ 0 & 0 & 0 & 1 \end{bmatrix},
$$

$$
{}^{\mathrm{B}'}_{\mathrm{M}}\mathbf{T} = \begin{bmatrix} \mathrm{c}\theta_2 & \mathrm{s}\theta_1\mathrm{s}\theta_2 & \mathrm{c}\theta_1\mathrm{s}\theta_2 & L_1\mathrm{c}\theta_1\mathrm{s}\theta_2 \\ 0 & \mathrm{c}\theta_1 & \mathrm{s}\theta_1 & L_1\mathrm{s}\theta_1 \\ -\mathrm{s}\theta_2 & \mathrm{s}\theta_1\mathrm{c}\theta_2 & \mathrm{c}\theta_1\mathrm{c}\theta_2 & L_1\mathrm{c}\theta_1\mathrm{c}\theta_2 \\ 0 & 0 & 0 & 1 \end{bmatrix}, \tag{1}
$$

$$
{}^{\mathrm{M}}_{\mathrm{M}'}\mathbf{T} = {}^{\mathrm{B}}_{\mathrm{B}'}\mathbf{T}^{-1},
$$

$$
{}^{\mathrm{M}'}_{\mathrm{U}}\mathbf{T} = \begin{bmatrix} \mathrm{c}\theta_3' & 0 & \mathrm{s}\theta_3' & L_2\mathrm{s}\theta_3' \\ 0 & 1 & 0 & 0 \\ -\mathrm{s}\theta_3' & 0 & \mathrm{c}\theta_3' & L_2\mathrm{c}\theta_3' \\ 0 & 0 & 0 & 1 \end{bmatrix}, \theta_3' = \theta_3 - \pi
$$

$$
{}^{\mathrm{O}}_{\mathrm{U}}\mathbf{T} = {}^{\mathrm{O}}_{\mathrm{B}}\mathbf{T}\,{}^{\mathrm{B}}_{\mathrm{B}'}\mathbf{T}\,{}^{\mathrm{B}'}_{\mathrm{M}}\mathbf{T}\,{}^{\mathrm{M}}_{\mathrm{M}'}\mathbf{T}\,{}^{\mathrm{M}'}_{\mathrm{U}}\mathbf{T}
$$

where $i = 1,\ 2,\ 3$ is the number of legs, and Rb, L_1, and L_2 are the radius of the base plate, length of the lower leg and the upper leg, respectively. With these homogeneous transformation matrices, the position vector from the B' frame to the spherical joint attached at the upper plate can be calculated like this.

$$-\frac{1}{\sqrt{2}}L_2\left(\mathrm{c}\theta_2\mathrm{s}\theta_3+\mathrm{s}\theta_1\mathrm{s}\theta_2\mathrm{s}\theta_3\right)-L_2\mathrm{c}\theta_1\mathrm{s}\theta_2\mathrm{c}\theta_3+L_1\mathrm{c}\theta_1\mathrm{s}\theta_2={}^{\mathrm{B}'}u_x$$

$$-\frac{1}{\sqrt{2}}L_2\mathrm{c}\theta_1\mathrm{s}\theta_3+L_2\mathrm{s}\theta_1\mathrm{c}\theta_3-L_1\mathrm{s}\theta_1={}^{\mathrm{B}'}u_y \quad (2)$$

$$-\frac{1}{\sqrt{2}}L_2\left(-\mathrm{s}\theta_2\mathrm{s}\theta_3+\mathrm{s}\theta_1\mathrm{c}\theta_2\mathrm{s}\theta_3\right)-L_2\mathrm{c}\theta_1\mathrm{c}\theta_2\mathrm{c}\theta_3+L_1\mathrm{c}\theta_1\mathrm{c}\theta_2={}^{\mathrm{B}'}u_z$$

The vector from the base to joint ${}^{i}_{O}\vec{\mathbf{U}}$ can be calculated with the ${}^{i}\theta_3$ and vector ${}^{i}_{O}\vec{\mathbf{M}}$ like this.

$${}^{i}_{O}\vec{\mathbf{U}}={}^{\mathrm{O}}_{\mathrm{B}}\mathbf{T}\;{}^{\mathrm{B}}_{\mathrm{B}'}\mathbf{T}\begin{bmatrix}{}^{\mathrm{B}'}u_x\\{}^{\mathrm{B}'}u_y\\{}^{\mathrm{B}'}u_z\\1\end{bmatrix} \quad (3)$$

The position vector and orientation matrix of the upper plate is expressed with 3 joint vectors ${}^{1}_{O}\vec{\mathbf{U}}$, ${}^{2}_{O}\vec{\mathbf{U}}$ and ${}^{3}_{O}\vec{\mathbf{U}}$ like this.

$$\vec{\mathbf{X}}=\frac{\left({}^{1}_{O}\vec{\mathbf{U}}+{}^{2}_{O}\vec{\mathbf{U}}+{}^{3}_{O}\vec{\mathbf{U}}\right)}{3}$$

$$\vec{\mathbf{d}}_{\mathrm{x}}=\frac{{}^{1}_{O}\vec{\mathbf{U}}}{\left\|{}^{1}_{O}\vec{\mathbf{U}}\right\|},\ \vec{\mathbf{d}}_{\mathrm{y}}=\frac{{}^{2}_{O}\vec{\mathbf{U}}-{}^{3}_{O}\vec{\mathbf{U}}}{\left\|{}^{2}_{O}\vec{\mathbf{U}}-{}^{3}_{O}\vec{\mathbf{U}}\right\|},\ \vec{\mathbf{d}}_{\mathrm{z}}=\vec{\mathbf{d}}_{\mathrm{x}}\times\vec{\mathbf{d}}_{\mathrm{y}} \quad (4)$$

Vector $\vec{\mathbf{X}}$ represents the position from the fixed coordinate center O to the upper plate center, and, $\vec{\mathbf{d}}_{\mathrm{x}}$, $\vec{\mathbf{d}}_{\mathrm{y}}$ and $\vec{\mathbf{d}}_{\mathrm{z}}$ are the direction cosines of the x, y and z axis, respectively.

3.2 Inverse position analysis

An inverse kinematics problem can be solved from the closed form forward kinematics equations.

First of all, ${}^{i}\theta_3$ can be calculated with this equation.

$$\cos{}^{i}\theta_3=-\frac{L_1^2+L_2^2-L^2}{2L_1L_2}$$

$$\text{where } L^2={}_{B}^{i}u_x^2+{}_{B}^{i}u_y^2+{}_{B}^{i}u_z^2 \quad (5)$$

${}^{i}\theta_1$ is calculated with the second equation in (2) as shown below

$$\tan{}^{i}\theta_1=\frac{-b_1+\sqrt{b_1^2+a_1^2-{}^{\mathrm{B}'}u_y^2}}{{}^{\mathrm{B}'}u_y-a_1}$$

$$a_1=\frac{L_2}{\sqrt{2}}\mathrm{s}\theta_3,\ b_1=\left(L_1\text{-}L_2\right)\mathrm{c}\theta_3 \quad (6)$$

The rotation angle ${}^{i}\theta_2$ about the y axis is expressed with the calculated ${}^{i}\theta_1$ and ${}^{i}\theta_3$,

$$\tan{}^{i}\theta_2=\frac{b_2\,{}^{\mathrm{B}'}u_x+a_2\,{}^{\mathrm{B}'}u_z}{b_2\,{}^{\mathrm{B}'}u_z-a_2\,{}^{\mathrm{B}'}u_x}$$

$$a_2=\frac{L_2}{\sqrt{2}}\mathrm{s}\theta_3,\ b_2=-\frac{L_2}{\sqrt{2}}\mathrm{s}\theta_1\mathrm{s}\theta_3-L_2\mathrm{c}\theta_1\mathrm{c}\theta_3+L_1\mathrm{c}\theta_1 \quad (7)$$

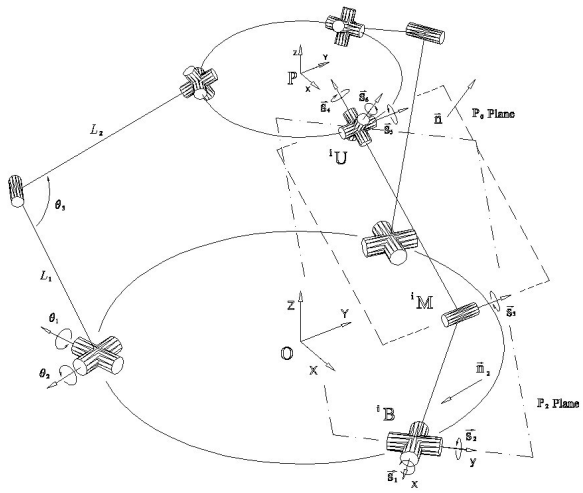

Fig. 4 Schematic diagram with a definition of the screw axes

3.3 Jacobian Analysis

Fig. 4 shows the schematic diagram with a definition of the screw axes. The twist of the upper plate is expressed as in this equation.

$$\hat{\mathbf{t}}={}^{i}\dot{\theta}_1\,{}^{i}\hat{\mathbf{S}}_1+{}^{i}\dot{\theta}_2\,{}^{i}\hat{\mathbf{S}}_2+{}^{i}\dot{\theta}_3\,{}^{i}\hat{\mathbf{S}}_3+{}^{i}\dot{\theta}_4\,{}^{i}\hat{\mathbf{S}}_4+{}^{i}\dot{\theta}_5\,{}^{i}\hat{\mathbf{S}}_5+{}^{i}\dot{\theta}_6\,{}^{i}\hat{\mathbf{S}}_6 \quad (8)$$

$\hat{\mathbf{t}}=\left[\ \vec{\mathbf{v}}^{\mathrm{T}}\ \vec{\boldsymbol{\omega}}^{\mathrm{T}}\ \right]^{\mathrm{T}}$ is the twist of upper plate. ${}^{i}\dot{\theta}_1$ and ${}^{i}\dot{\theta}_2$ are the angular velocities of the active joints of the i th leg, and the others are passive ones. The angular velocities of the passive joints can not be measured directly. Using the concept of reciprocal screws, these velocity terms can be removed.

Two screws $\hat{\mathbf{S}}_p$ and $\hat{\mathbf{S}}_q$ are said to be reciprocal if

$$\hat{\mathbf{S}}_p^{\mathrm{T}}\hat{\mathbf{S}}_q=0,\ p\neq q \quad (9)$$

where $\hat{\mathbf{S}}_p^{\mathrm{T}}$ is defined as $\left[\ s_4\ s_5\ s_6\ s_1\ s_2\ s_3\ \right]^{\mathrm{T}}$ and is transpose of a screw $\hat{\mathbf{S}}_p=\left[\ s_1\ s_2\ s_3\ s_4\ s_5\ s_6\ \right]^{\mathrm{T}}$.

Since there is a spherical joint at the upper plate and a revolute joint at the middle, all the screws are reciprocal to the unactuated joint screws which form a planar pencil. Specifically, all the reciprocal screws are zero-pitch screws passing through ${}^{\mathrm{i}}\mathrm{U}$ and lying on a plane P_0 that contains the axis of $\hat{\mathbf{S}}_3$ and point ${}^{\mathrm{i}}\mathrm{U}$.

Let ${}^{i}\vec{\mathbf{n}}$, ${}^{i}\vec{\mathbf{n}}_1$ and ${}^{i}\vec{\mathbf{n}}_2$ be the normal vectors of each plane, respectively.

$${}^{i}\vec{\mathbf{n}}={}^{i}\vec{\mathbf{s}}_3\times{}^{i}\vec{\mathbf{s}}_4,\ {}^{i}\vec{\mathbf{n}}_1={}^{i}\vec{\mathbf{s}}_2\times{}^{i}\vec{\mathbf{u}},\ {}^{i}\vec{\mathbf{n}}_2={}^{i}\vec{\mathbf{s}}_1\times{}^{i}\vec{\mathbf{u}} \quad (10)$$

Then the screws that are reciprocal to all the screws except for $\hat{\mathbf{S}}_1$ are obtained by an intersection of the P_0-plane and P_1- plane that passes point ${}^{\mathrm{i}}\mathrm{U}$ and contains the axes of $\hat{\mathbf{S}}_1$.

$$
{}^{i}\hat{\mathbf{\$}}_{1r}=\begin{bmatrix} {}^{i}\vec{\mathbf{s}}_{1r} \\ {}^{i}\vec{\mathbf{s}}_{10r} \end{bmatrix},\ \text{where } {}^{i}\vec{\mathbf{s}}_{1r}={}^{i}\vec{\mathbf{n}}\times{}^{i}\vec{\mathbf{n}}_{1},\ {}^{i}\vec{\mathbf{s}}_{10r}={}^{i}\vec{\mathbf{U}}_{\mathrm{O}}\times{}^{i}\vec{\mathbf{s}}_{1r}
$$
$$
{}^{i}\hat{\mathbf{\$}}_{2r}=\begin{bmatrix} {}^{i}\vec{\mathbf{s}}_{2r} \\ {}^{i}\vec{\mathbf{s}}_{20r} \end{bmatrix},\ \text{where } {}^{i}\vec{\mathbf{s}}_{1r}={}^{i}\vec{\mathbf{n}}\times{}^{i}\vec{\mathbf{n}}_{2},\ {}^{i}\vec{\mathbf{s}}_{20r}={}^{i}\vec{\mathbf{U}}_{\mathrm{O}}\times{}^{i}\vec{\mathbf{s}}_{2r} \tag{11}
$$

The twist of the upper plate can be simplified like these.

$$
\begin{aligned}
{}^{i}\hat{\mathbf{\$}}_{1r}^{\mathrm{T}}\hat{\mathbf{t}}&={}^{i}\dot{\theta}_{1}\,{}^{i}\hat{\mathbf{\$}}_{1r}^{\mathrm{T}}\,{}^{i}\hat{\mathbf{\$}}_{1} \\
{}^{i}\hat{\mathbf{\$}}_{2r}^{\mathrm{T}}\hat{\mathbf{t}}&={}^{i}\dot{\theta}_{2}\,{}^{i}\hat{\mathbf{\$}}_{2r}^{\mathrm{T}}\,{}^{i}\hat{\mathbf{\$}}_{2}
\end{aligned} \tag{12}
$$

Rearranging the expressions for the twist of the upper plate into a matrix form,

$$
\dot{\boldsymbol{\theta}}=\mathbf{j}^{\mathrm{T}}\hat{\mathbf{t}} \tag{13}
$$

where $\mathbf{j}^{\mathrm{T}}=\begin{bmatrix} \frac{{}^{1}\hat{\mathbf{\$}}_{1r}}{{}^{1}\vec{\mathbf{s}}_{1r}^{\mathrm{T}}\,{}^{1}\vec{\mathbf{s}}_{1}} & \frac{{}^{1}\hat{\mathbf{\$}}_{2r}}{{}^{1}\vec{\mathbf{s}}_{2r}^{\mathrm{T}}\,{}^{1}\vec{\mathbf{s}}_{2}} & \frac{{}^{2}\hat{\mathbf{\$}}_{1r}}{{}^{2}\vec{\mathbf{s}}_{1r}^{\mathrm{T}}\,{}^{2}\vec{\mathbf{s}}_{1}} & \frac{{}^{2}\hat{\mathbf{\$}}_{2r}}{{}^{2}\vec{\mathbf{s}}_{2r}^{\mathrm{T}}\,{}^{2}\vec{\mathbf{s}}_{2}} & \frac{{}^{3}\hat{\mathbf{\$}}_{1r}}{{}^{3}\vec{\mathbf{s}}_{1r}^{\mathrm{T}}\,{}^{3}\vec{\mathbf{s}}_{1}} & \frac{{}^{3}\hat{\mathbf{\$}}_{2r}}{{}^{3}\vec{\mathbf{s}}_{2r}^{\mathrm{T}}\,{}^{3}\vec{\mathbf{s}}_{2}} \end{bmatrix}^{\mathrm{T}}$

$\mathbf{j}^{\mathrm{T}}$ is a (6×6) matrix which represents a kinematic Jacobian.

4. Optimal Design

4.1 Performance Index

A good haptic device exerts a uniformly distributed force, and has a high sensitivity. In a previous work [8], the isotropic index, or shape index is defined as the ratio of the minimum singular value to the maximum singular value of the Jacobian matrix. But this index is not invariant under a change of a unit due to the unit discordance of the Jacobian matrix. So, the isotropic index in this work is defined from the force transmission analysis of Hansung Kim [9]. The isotropic index for the force is defined like this,

$$
\mathrm{II}_{\mathrm{f}}\equiv\frac{\alpha_{f\min}}{\alpha_{f\max}},\ 0\le\mathrm{II}_{\mathrm{f}}\le 1, \tag{14}
$$

where, $\alpha_{f\max}$ and $\alpha_{f\min}$ are the maximum and minimum value of the eigenvalues of $\mathbf{j}\mathbf{j}^{\mathrm{T}}$. This index provides a measure of the shape of the force transmission ellipsoid. The II_{f} becomes closer to unity, the device can exert a more uniform force in every direction.

When the input motor torques have a unity magnitude, the extreme values of the payload at the end-effector is defined as the payload index. And mathematically, the payload index is expressed by the maximum eigenvalue of the Jacobian matrix. A large payload index means that a device requires smaller actuators to exert the same end-effector payload.

$$
\mathrm{PI}_{\mathrm{f}}\equiv\alpha_{f\max} \tag{15}
$$

Using the same manner, the isotropic index for a moment and the payload index for a moment are defined like this.

$$
\begin{aligned}
&\mathrm{II}_{\mathrm{m}}\equiv\frac{\alpha_{m\min}}{\alpha_{m\max}},\ 0\le\mathrm{II}_{\mathrm{m}}\le 1 \\
&\mathrm{PI}_{\mathrm{m}}\equiv\alpha_{m\max}
\end{aligned} \tag{16}
$$

4.2 Global Performance Index

The isotropic index and payload index are calculated from the eigenvalue problems of the Jacobian matrix. But, the Jacobian matrix is dependent on the position and orientation of the end-effector. Hence, it requires a global index which can represent the performance of the mechanism in the whole workspace.

The global isotropic index and global payload index are defined as below:

$$
\mathrm{GII}_{\mathrm{f,m}}\equiv\frac{\int_{V}\mathrm{II}_{\mathrm{f,m}}d\mathrm{v}}{\int_{\mathrm{V}}d\mathrm{v}},\quad \mathrm{GPI}_{\mathrm{f,m}}\equiv\frac{\int_{V}\mathrm{PI}_{\mathrm{f,m}}d\mathrm{v}}{\int_{\mathrm{V}}d\mathrm{v}}, \tag{17}
$$

where, $d\mathrm{v}$ means the infinitesimal volume, and $\mathrm{II}_{\mathrm{f,m}}$ and $\mathrm{PI}_{\mathrm{f,m}}$ mean the isotropic index for a force and moment, and a payload index for a force and moment measured at the center of the infinitesimal volume, respectively. It is required to define a design index to optimize the design parameters of the mechanism to get a good performance. To define a design index, global indices are normalized to make the dimensionless.

$$
\begin{aligned}
\mathrm{GII}_{\mathrm{f,m(norm)}}&\equiv\frac{\mathrm{GII}_{\mathrm{f,m}}-\mathrm{GII}_{\mathrm{f,m(min)}}}{\mathrm{GII}_{\mathrm{f,m(max)}}-\mathrm{GII}_{\mathrm{f,m(min)}}} \\
\mathrm{GPI}_{\mathrm{f,m(norm)}}&\equiv\frac{\mathrm{GPI}_{\mathrm{f,m}}-\mathrm{GPI}_{\mathrm{f,m(min)}}}{\mathrm{GPI}_{\mathrm{f,m(max)}}-\mathrm{GPI}_{\mathrm{f,m(min)}}}
\end{aligned} \tag{18}
$$

4.3 Optimization using genetic algorithms

To caculate the optimal mechanical parameters, the objective function is defined as Eq. 19

$$
\begin{aligned}
\text{maximize GDI}=\min[&\mathrm{GII}_{f(norm)},\mathrm{GII}_{m(norm)}, \\
&\mathrm{GPI}_{f(norm)},\mathrm{GPI}_{m(norm)},\mathrm{WS}_{norm}]
\end{aligned} \tag{19}
$$

where GDI is the global design index and WS_{norm} is the norm value of the workspace.

In solving the objective function, the range of the mechanical parameters is defined as in Table 1.

Table 1. The range of the mechanical parameters

Parameter	Min[mm]	Max[mm]
Radius of the moving plate	40	60
Radius of the base plate	40	60
Length of the lower leg	110	130
Length of the upper leg	150	170

Because of the high nonlinearity of the objective function, a global optimization is needed. Genetic Algorithms [10] are adopted for the global optimization technique. And the radius of the base plate, moving plate, lengths of the upper and lower legs are taken to design the parameters to maximize the global design index.

The results of the optimization are shown in tables 1~2. Fig. 5 shows the reachable workspace of this proposed device, and Fig.6. shows the optimal designed mechanism.

Table 2. Results of the Genetic Algorithms

design parameters	optimal values [mm]
Radius of the moving plate	57.3
Radius of the base plate	57.0
Length of the lower leg	117.0
Length of the upper leg	154.1

Table 3. The results values of the indexs

	min	result	max
GDI		0.5039	
$GII_{f(norm)}$	0.4104	0.5413	0.6702
$GII_{m(norm)}$	0.5275	0.5820	0.6176
$GPI_{f(norm)}$	13.3102	16.2123	19.0692
$GPI_{m(norm)}$	0.4445	0.7633	0.9199
WS_{norm} [cm^3]	10.6113	16.8373	22.8270

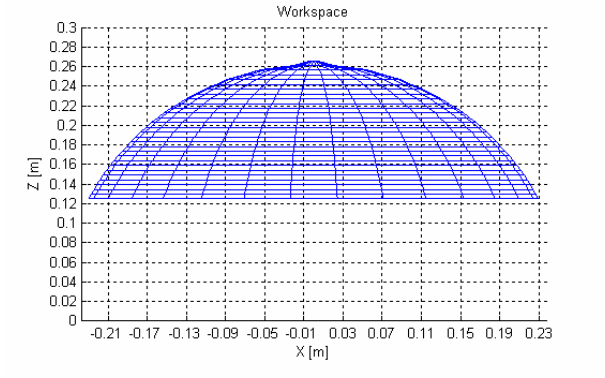

Fig. 5 Reachable workspace of the proposed device

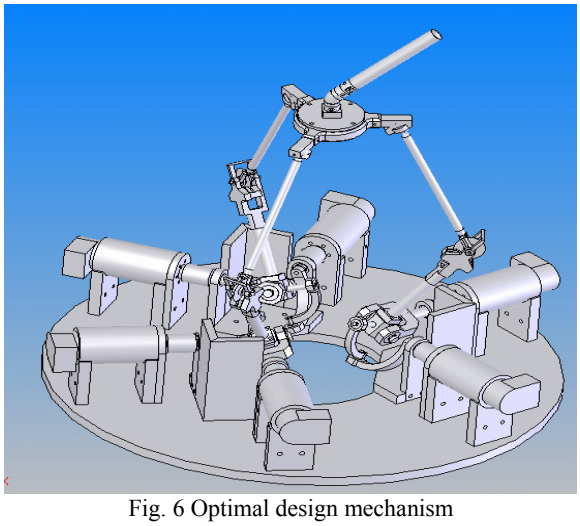

Fig. 6 Optimal design mechanism

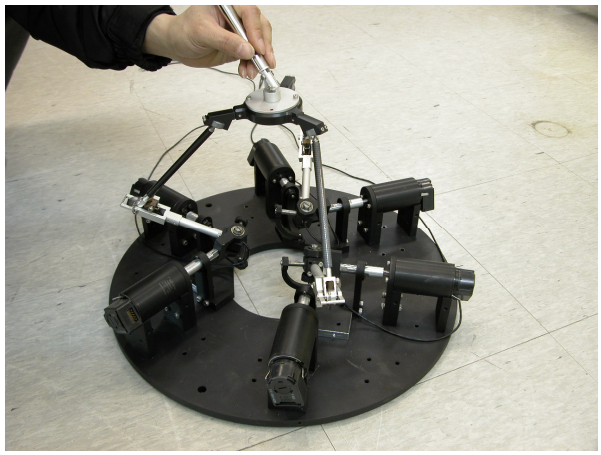

Fig. 7 The figure of the proposed haptic device

In Fig. 5, the reachable workspace covers the requirement (160W, 120H, 120D).

Using the above results and the conceptual design, the proposed haptic device is manufactured as in Fig. 6.

5. Conclusion

In this work, this paper proposed a new haptic device using a parallel mechanism with gimbal type actuators. This device has three legs actuated by 2-DOF gimbal mechanisms, which make the device simple and light by fixing all the actuators to the base. Three extra sensors are placed at passive joints to obtain a unique solution of the forward kinematics problem.

The proposed haptic device is developed for an operator to use it on a desktop in due consideration of the size of an average Korean. With this conceptual design, an optimization of the design parameters is carried out. The objective function is defined by the fuzzy minimum of the global design indices – global force/moment isotropy index, global force/moment payload index, and workspace. Each global index is calculated by a SVD (singular value decomposition) of the force and moment parts of the jacobian matrix. Division of the jacobian matrix assures a consistency of the units in the matrix. Due to the nonlinearity of this objective function, Genetic algorithms is adopted for a global optimization.

The proposed haptic device has a small workspace for an operator to use it on a desktop and more sensitivity than a serial type haptic device. Therefore, the motors of the proposed haptic device are fixed at the base plate so that the proposed haptic device has a better dynamic bandwidth due to a low moving inertia.

On the basis of the results of an optimization, we manufactured the new haptic device.

ACKNOWLEDGMENTS

This work was performed under the long-term nuclear R&D program sponsored by the Korea Ministry of Science and Technology.

REFERENCES

[1] R. C. Goertz, "Fundamentals of general-purpose remote manipulators," *Nucleonics*, Vol. 10, No. 11, pp. 36-42, 1962.

[2] M. Bergamasco, et al., "An arm exoskeleton system for

teleoperation and virtual environments applications," *Proc. 1994 IEEE Int. Conf. on Robotics and Automation*, San Diego, California, pp. 1449-1454.

[3] T. H. Massie and J. K. Salisbury, "The PHANToM haptic interfaces: A device for probing virtual objects," *Proc. of the 1994 ASME Int. Mechanical Engineering Exposition and Congress*, Chicago, Illinois, pp. 295-302, 1994.

[4] Kiyoung Woo, Byoungdae Jin, and Dong-soo Kwon, "A 6 DOF force-reflecting hand controller using the fivebar parallel mechanism," *Proc. 1998 IEEE Int. Conf. on Robotics and Automation*, Leuven, Belgium, pp.1597-1602, 1998.

[5] Jungwon Yoon and Jeha Ryu, "Design and analysis of a new haptic device using a parallel mechanism," *Proc. 2000 IEEE/RSJ Int. Conf. on Intelligent Robots and Systems*, pp. 949-954, 2000.

[6] Lee, J. H., K. S. Eom, B-J Yi, and I. H. Suh, "Design of a new 6-DOF parallel haptic device," *Proc. 2001 IEEE Int. Conf. on Robotics and Automation*, pp.886-891, 2001.

[7] Y. Tsumaki, H. Naruse, D. N. Nenchev, and M. Uchiyama, "Design of a compact 6-DOF haptic interface," *Proc. 1998 IEEE Int. Conf. on Robotics and Automation*, Leuven, Belgium, pp.2580-2585, 1998.

[8] Byung-Ju Yi, Daniel Cox, and Delbert Tesar, "Analysis and design criteria for a redundantly actuated 4-legged six Degree-of-Freedom parallel manipulator," *Proc. 2001 IEEE Int. Conf. on Robotics and Automation*, Seoul, Korea, pp. 3286-3293, 2001.

[9] Hansung Kim, "Design and control of a stewart platform based machine tool," Ph.d thesis, 1999

[10] Deb, K., "Genetic algorithm in search and optimization: The technique and applications," *Proc. of Int. Workshop on Soft Computing and Intelligent Systems,* Calcutta, India, pp. 58-87, 1998.